

# Learned Inertial Odometry for Cycling Based on Mixture of Experts Algorithm

Hao Qiao<sup>a</sup>, Yan Wang<sup>b,\*</sup>, Shuo Yang<sup>c</sup>, Xiaoyao Yu<sup>a</sup>, Jian kuang<sup>b</sup>, Xiaoji Niu<sup>b,c</sup>

<sup>a</sup>School of Geodesy and Geomatics, Wuhan University, Wuhan, 430079, China

<sup>b</sup>GNSS Research Center, Wuhan University, Wuhan, 430079, China

<sup>c</sup>Hubei Luojia Laboratory, Wuhan University, Wuhan, 430079, China

## Abstract

With the rapid growth of bike sharing and the increasing diversity of cycling applications, accurate bicycle localization has become essential. traditional GNSS-based methods suffer from multipath effects, while existing inertial navigation approaches rely on precise modeling and show limited robustness. Tight Learned Inertial Odometry (TLIO) achieves low position drift by combining raw IMU data with predicted displacements by neural networks, but its high computational cost restricts deployment on mobile devices. To overcome this, we extend TLIO to bicycle localization and introduce an improved Mixture-of Experts (MoE) model that reduces both training and inference costs. Experiments show that, compared to the state-of-the-art LLIO framework, our method achieves comparable accuracy while reducing parameters by 64.7% and computational cost by 81.8%.

**Keywords:** Cycling Navigation, Inertial State Estimation, AI-Based Method, Mixture of Experts (MoE)

## 1. Introduction

Bicycles, due to their advantages of being environmentally friendly, flexible, and convenient, are widely used in transportation, rehabilitation training, military operations, and sports. As applications expand, the demand for high-precision localization has grown rapidly. The recent proliferation of bike sharing systems has further underscored the importance of efficient localization for effective fleet management.

Currently, bicycle location relies mainly on the Global Navigation Satellite System (GNSS). GNSS has been extensively adopted in commercial cycling devices (e.g. Garmin Edge) due to its all-weather availability, low cost, and high accuracy. However, in environments such as urban canyons, tunnels and tree-covered roads, GNSS signals are vulnerable to blockage and multipath effects, leading to severe degradation or even failure in positioning accuracy. Consequently, GNSS alone cannot provide stable and continuous localization in complex scenarios.

Inertial Navigation Systems (INS) offer self-contained localization without requiring external signals. With the rapid development of Micro-Electro-Mechanical Systems (MEMS), low-cost IMUs have been widely integrated into smartphones and wearable devices. However, INS suffers from error accumulation and substantial noise in low-cost IMUs, necessitating the use of motion constraints or external aiding information. In bicycle localization, methods inspired by Pedestrian Dead Reckoning (PDR), such as wheel constraints (CDR)[1] and nonholonomic constraints (NHC)[10], have been proposed. However, these approaches heavily rely on physical modeling and lack robustness in different types of bicycle.

Recently, data-driven inertial odometry has shown promising advantages over traditional methods. IONet[2] was the first to employ an LSTM network to estimate relative displacement on the ground plane. RoNIN[4] fused acceleration, angular velocity, and magnetic field data to infer global orientation and then applied deep networks (ResNet, LSTM, TCN) for velocity estimation. IDOL jointly learned orientation and position and achieved higher accuracy. TLIO[5] tightly integrated deep networks with a Kalman filter to enable 3D pose estimation in complex scenarios. CTIN[6] leveraged self-attention to capture both local and global context and improved feature representation. Collectively, these studies demonstrated strong accuracy and robustness across diverse motion patterns and provided valuable guidance for advancing bicycle inertial odometry.

Despite these advances, the computational cost of data-driven methods remains a major bottleneck for deployment on mobile platforms. For example, TLIO achieves high accuracy with ResNet-based feature extraction but incurs heavy inference overhead. To address this limitation, lightweight architectures have been proposed: LLIO employs a compact MLP to enhance efficiency without sacrificing accuracy, while ResMixer replaces convolutional layers with Mixer layers to reduce computational load while preserving feature interactions. More recently, sparsely Mixture-of-Experts (MoE)[7] frameworks have improved scalability and efficiency through routing and load-balancing mechanisms. The shared-expert isolating strategy in DeepSeekMoE[3], for instance, captures common knowledge while avoiding redundancy, thereby maintaining stability under constrained computational resources. These advances suggest that integrating improved MoE models into learning-based inertial odometry may achieve a better trade-off among accuracy, efficiency, and resource consumption.

\*Corresponding author

In this work, we present a lightweight learned inertial odometry for bicycles based upon a Mixture-of-Experts (MoE) model. The proposed approach provides 3D dead reckoning with low parameter count and computational cost. The main contributions of this work are:

- **Innovative application of learned inertial odometry for cycling.** This work innovatively applies learned inertial odometry to bicycles, overcoming the limitations of traditional physics-based methods that struggle with the vehicle’s high degrees of freedom.
- **Lightweight MoE-based architecture.** We adopt a MoE-based architecture that significantly reduces both parameter size and computational cost compared with current state-of-the-art methods.

## 2. System Overview

The proposed system takes raw IMU measurements together with orientation as inputs and produces a three-dimensional state estimate relative to the first instance. As shown in Fig. The system is composed of two primary components: an error-state Extended Kalman filter, and a lightweight inertial odometry network model based on a Mixture of Experts (MoE) framework.

The Kalman filter performs mechanization using raw IMU measurements and applies measurement updates with the output of the MoE model. By tightly coupling raw IMU measurements with the velocity estimated by the MoE model, the filter enables joint estimation of orientation, velocity, position, and IMU biases.

The MoE model takes a sequence of IMU measurements and orientation for velocity estimation. Specifically, based on the IMU measurements in the body frame and the orientation provided by the filter, the MoE model estimates the three-dimensional body-frame velocity at the end moment of the window along with the associated covariance matrix. The MoE model performs inference every 0.1 seconds, using a two-second sequence of IMU measurements and orientation as input.

In the proposed system, the IMU measurements are utilized in two distinct ways. First, within the filter, raw IMU measurements are employed for the IMU mechanization to obtain prior estimates of orientation, velocity, and position. Second, IMU measurements combined with orientation are input to the MoE model to produce velocity estimates with covariance, which serve as measurement updates for the filter. The latter essentially treats IMU measurements as motion indices, mapping IMU–orientation sequences to velocity through the learned correlations within the MoE model. This design avoids redundant use of IMU data.

## 3. Algorithm Description

### 3.1. MoE model

This section introduces the MoE model proposed in the algorithm and Fig illustrates the framework of the MoE model.

#### 3.1.1. Network architecture

The architecture of the MoE model is composed of two main components: the gating network and the expert networks, which are described separately below.

In the MoE framework, the gating network determines a small subset of  $K$  experts to be activated for each input sample. This selective activation preserves the expressive capacity of the model while significantly reducing computational overhead, making the gating mechanism a critical component. As illustrated in fig.2, the model employs a shared-expert-freezing strategy following the design of DeepSeekMoE[3], where a shared expert is always activated to process all samples. To further improve efficiency, the remaining experts are activated according to a Top- $K$  selection rule. Specifically, for each batch of input, the gating network ranks the expert scores and selects the top  $K$  experts with the highest weights for inference, while discarding the rest.

The gating network is implemented as follows: each sample passes sequentially through a convolutional layer, an activation layer, a global average pooling layer, and a linear layer to generate expert-specific weights. These weights are normalized via a softmax layer to form a probability distribution. For each sample, the top  $K$  experts with the highest probabilities are chosen, their probabilities are renormalized, and a sparse one-hot gating matrix is constructed to allocate samples to the corresponding experts.

The expert network adopts LLIO-net[9] as the backbone for feature extraction, which is mainly built upon the ResMLP[8] structure. The design consists of three modules: a feature convert module, a ResMLP module, and a regression module. The feature convert module reorganizes the raw input into feature matrices, the ResMLP module extracts high-level representations, and the regression module integrates features from both the shared expert and the Top- $K$  experts to jointly predict velocity and the associated covariance.

However, in the MoE architecture, if all inputs are routed to only a few experts, the training efficiency will be greatly reduced, and the model will gradually degenerate from a mixture-of-experts into an equivalent single-expert network. This occurs because when the gating network tends to select a few fixed experts, the corresponding weight vectors of these experts increase during backpropagation, making it difficult for the other experts to contribute.

To mitigate this issue, we introduce an *expert capacity* (Capacity) constraint in the gating network to optimize load balancing among experts. The expert capacity is defined as:

$$\text{Capacity}_i = \left\lceil \frac{c \times B}{N} \right\rceil \quad (1)$$

where  $\lceil \cdot \rceil$  denotes the ceiling operation. This formulation ensures that, within a batch of data, each expert can receive at most  $\frac{c \times B}{N}$  inputs. If the number of inputs assigned to a certain expert exceeds this limit, the excess inputs are reassigned to the expert with the next highest weight. If that expert also exceeds its capacity, the input is passed further down to subsequent experts in descending order of their weights.

The input to the feature extraction module consists of raw IMU measurements and the corresponding orientations from time  $t - L$  to  $t$ , forming a  $9 \times L$  matrix. In the feature convert module, the input is divided into  $N_{\text{patch}}$  patches, each containing  $L_{\text{feature}}$  measurements, where  $L = N_{\text{patch}} \times L_{\text{feature}}$ . Each patch is then flattened and all the features are concatenated to obtain  $N_{\text{patch}}$  embeddings of dimension  $(9 \times L_{\text{feature}})$ . These  $N_{\text{patch}}$  embeddings are then fed into the ResMLP module.

The ResMLP module consists of two components: a cross-patch interaction module and a cross-channel interaction module. Before entering the ResMLP, a linear layer maps the input from dimension  $N_{\text{patch}} \times (9 \times L_{\text{feature}})$  to  $N_{\text{patch}} \times L_{\text{inner-feature}}$ .

In the cross-patch interaction module, the input is sequentially passed through an affine layer, a one-dimensional convolutional layer, a linear layer, and another affine layer. Here, the affine layer serves as an alternative to layer normalization, performing element-wise scaling and shifting on the input. The affine operation is defined as:

$$\text{AFF}_{\alpha, \beta}(x) = \text{Diag}(\alpha) x + \beta \quad (2)$$

where  $\alpha$  and  $\beta$  are learnable parameters. It should be noted that when  $\text{AFF}(\cdot)$  is applied to a matrix, the operation is performed independently on each column. To facilitate multilayer stacking, both the convolutional and linear layers preserve the input dimension, which requires the convolution kernel size to be set to 1.

In the cross-channel interaction module, the data sequentially pass through a linear layer, an activation function layer, and another linear layer. The second linear layer maps the representation from  $N_{\text{patch}} \times L_{\text{inner-feature}}$  to  $N_{\text{patch}} \times L_{\text{out-dim}}$ .

The regression module concatenates the weighted features extracted by the Top-K experts with those extracted by the shared expert and then fuses them through a linear layer. This fused representation is further processed by a global average pooling layer, followed by a linear layer and an activation function layer for feature transformation. Finally, two separate linear layers are employed to estimate two three-dimensional vectors: the velocity and the diagonal elements of the covariance matrix.

### 3.1.2. Training Methodology

The training of the MoE model is primarily based on three loss functions:

- **Mean Squared Error (MSE) Loss:** applied to the predicted velocity  $\hat{v}^b$ .
- **Negative Log-Likelihood (NLL) Loss:** applied jointly to  $\hat{v}^b$  and its covariance  $\Sigma_{\hat{v}^b}$ .
- **Auxiliary Balancing Loss:** used to encourage balanced utilization across experts.

The mean squared error (MSE) loss is defined as:

$$\mathcal{L}_{\text{MSE}}(v, \hat{v}) = \frac{1}{n} \sum \|v - \hat{v}\|^2 \quad (3)$$

where  $v^b$  denotes the ground truth velocity in the body frame, and  $\hat{v}^b$  is the velocity predicted by the MoE model. Through minimize  $\mathcal{L}_{\text{MSE}}$ , the MoE model learns to predict the three-dimensional velocity.

The negative log-likelihood (NLL) loss is defined as:

$$\mathcal{L}_{\text{NLL}}(v, \hat{v}, \hat{\Sigma}) = \frac{1}{n} \sum \left( \frac{1}{2} \log \det \hat{\Sigma} + \frac{1}{2} \|v - \hat{v}\|_{\hat{\Sigma}}^2 \right) \quad (4)$$

where  $\hat{\Sigma}_{\hat{v}^b}$  denotes the covariance matrix corresponding to the predicted velocity  $\hat{v}^b$ . The Mahalanobis distance  $\|v - \hat{v}\|_{\hat{\Sigma}}^2$  is defined as:

$$\|v - \hat{v}\|_{\hat{\Sigma}}^2 = (v - \hat{v})^T \hat{\Sigma} (v - \hat{v}) \quad (5)$$

Through minimize  $\mathcal{L}_{\text{NLL}}$ , the MoE model learns to predict the three-dimensional velocity.

The auxiliary balancing function is designed to encourage a balanced allocation of outputs across experts. It is implemented as follows: for a batch of  $B$  inputs, the importance of expert  $i$ , denoted as  $I_i$ , is defined as the sum of the expert weight vectors received by this expert over the entire batch:

$$I_i = \sum_{t=1}^B g_i(x_t) \quad (6)$$

where  $g_i(x)$  denotes the gating weight generated by the gating network for input  $x$  with respect to expert  $i$ . Ideally, the importance of each expert should be uniformly distributed across all experts, i.e.,

$$I_i \approx \frac{1}{N} \sum_{j=1}^N I_j \quad (7)$$

Similarly, in addition to considering the continuous probability distribution, the actual number of times each expert is selected should also be taken into account. The load of expert  $i$ , denoted as  $L_i$ , is defined as:

$$L_i = \sum_{t=1}^B \mathbf{I}(i \in S(x_t)) \quad (8)$$

where  $\mathbf{I}(\cdot)$  is the indicator function, and  $S(x)$  denotes the set of experts assigned to input  $x$ . Ideally, the load distribution across experts should be approximately uniform, i.e.,

$$L_i \approx \frac{B}{N} \quad (9)$$

Based on the above, to encourage balanced allocation of input data among experts, the importance loss and load loss can be formulated as follows:

$$\begin{aligned} \mathcal{L}_{\text{importance}} &= \sum_{i=1}^N \left( \frac{I_i}{\sum_{j=1}^N I_j} - \frac{1}{N} \right)^2 \\ \mathcal{L}_{\text{load}} &= \sum_{i=1}^N \left( \frac{L_i}{\sum_{j=1}^N L_j} - \frac{1}{N} \right)^2 \end{aligned} \quad (10)$$

The importance loss measures the deviation of the experts' importance distribution from a uniform distribution. After normalizing the importance of each expert, it is compared with

the ideal uniform value  $1/N$ , and larger deviations incur higher loss. The load loss encourages the number of times each expert is selected to be close to the mean, preventing certain experts from being over-utilized. The overall auxiliary balancing loss combines these two components as follows:

$$\mathcal{L}_{aux} = \mathcal{L}_{importance} + \mathcal{L}_{load} \quad (11)$$

By minimizing  $\mathcal{L}_{aux}$ , the importance and load distributions are encouraged to be close to uniform. This prevents certain experts from being over-utilized or under-utilized, leading to a more balanced distribution of importance and load among experts. Consequently, the MoE model can effectively leverage the diverse expertise of all experts while maintaining computational efficiency and training stability.

During the training process, the MoE model is first trained by minimizing  $\mathcal{L}_{MSE} + \lambda \mathcal{L}_{aux}$  until convergence. Subsequently,  $\hat{v}_t^b$  and  $\Sigma_{\hat{v}_t^b}$  are jointly trained by minimizing  $\mathcal{L}_{NLL} + \lambda \mathcal{L}_{aux}$  until convergence, where  $\lambda$  is the weighting coefficient for the auxiliary balancing loss.

### 3.2. Extended Kalman filter

The MoE model predicts velocity in the body frame, enabling direct constraints on the current frame without the need to track historical states, thus simplifying the filter architecture.

#### 3.2.1. System State Definition

The system state of the Extended Kalman Filter (EKF) is defined as:

$$X_t = (R_t, v_t^n, p_t^n, b_{g,t}, b_{a,t}) \quad (12)$$

where  $b_{gt}$  and  $b_{at}$  denote the biases of the gyroscope and accelerometer, respectively. The Kalman filter in this work is formulated based on the error of the system state, which is defined as:

$$\delta X_t = (\phi_t, \delta v_t^n, \delta p_t^n, \delta b_{g,t}, \delta b_{a,t}) \quad (13)$$

where  $\phi_t$  is a  $3 \times 1$  vector representing the attitude error, defined as:

$$\phi_t = \log_{SO(3)}(R_t \hat{R}_t^{-1}) \quad (14)$$

where  $\log_{SO(3)}$  denotes the logarithmic map from the Lie group  $SO(3)$  to its Lie algebra  $\mathfrak{so}(3)$ .

#### 3.2.2. State Propagation

The filter employs a simplified kinematic formulation for state propagation:

$$\begin{aligned} \hat{R}_{t+1} &= \hat{R}_t \exp_{SO(3)}(\omega_{ib,t}^b - \hat{b}_{g,t}) \\ \hat{v}_{t+1}^n &= \hat{v}_t^n + g \Delta t + R_t f_t^b \Delta t - \hat{b}_{a,t} \Delta t \\ \hat{p}_{t+1}^n &= \hat{p}_t^n + 0.5 (\hat{v}_t^n + \hat{v}_{t+1}^n) \Delta t \\ \hat{b}_{g,t+1} &= \hat{b}_{g,t} \quad \hat{b}_{a,t+1} = \hat{b}_{a,t} \end{aligned} \quad (15)$$

Here,  $\exp_{SO(3)}$  denotes the exponential map from the Lie algebra  $\mathfrak{so}(3)$  to the Lie group  $SO(3)$ . The linearized propagation model of the error state is given by:

$$\delta \hat{X}_{t+1} = A_t \delta \hat{X}_t + B_t n_t \quad (16)$$

where  $n_t = (n_{gt} \ n_{at} \ \eta_{bgt} \ \eta_{bat})^T$  represents the noise of the gyroscope and accelerometer, as well as the random walk noise of their biases. The corresponding covariance propagation model is given by:

$$P_{t+1} = A_t P_t A_t^T + B_t Q_t B_t^T \quad (17)$$

where  $P_t$  and  $Q_t$  denote the covariance matrices of the system state and the noise at time  $t$ , respectively.

#### 3.2.3. Measurement Update

The measurement update is as follows:

$$h(X_t) = \hat{R}_t^T v_t^n = \hat{v}_t^b + n_{\hat{v}_t^b} \quad (18)$$

where  $n_{\hat{v}_t^b}$  follows a Gaussian distribution  $\mathcal{N}(0, \Sigma_{\hat{v}_t^b})$ . The function  $h(X_t)$  has nonzero partial derivatives only with respect to  $\hat{\phi}_t$  and  $\delta v_t^n$ . The corresponding Jacobian matrix is given by:

$$\begin{aligned} H(\hat{\phi}_t) &= \frac{\partial h(X)}{\partial \hat{\phi}_t} = \hat{R}_t^T (\hat{v}_t^n)_{\times} \\ H(\delta \hat{v}_t^n) &= \frac{\partial h(X)}{\partial \delta \hat{v}_t^n} = \hat{R}_t^T \end{aligned} \quad (19)$$

Finally, the Kalman Gain and the update can be computed as follows:

$$\begin{aligned} K_t &= P_t H_t^T (H_t P_t H_t^T + \Sigma_{\hat{v}_t^b})^{-1} \\ \hat{X}_t &\leftarrow \hat{X}_t \oplus (K_t (h(X_t) - \hat{v}_t^b)) \\ P_t &= (I - K_t H_t) P_t (I - K_t H_t)^T + K_t \Sigma_{\hat{v}_t^b} K_t^T \end{aligned} \quad (20)$$

Here,  $\oplus$  denotes the operation of adding the error state to the system state. It should be noted that the attitude update is computed as  $\hat{R}_t = \exp_{SO(3)}(\hat{\phi}_t) \hat{R}_t^-$ .

## 4. experiments

### 4.1. Set Up

#### 4.1.1. Dataset

The dataset was collected using a self-developed data acquisition application capable of accessing the smartphone's built-in IMU, GNSS, magnetometer, and Wi-Fi sensors. During data collection, the smartphone was securely mounted on the bicycle handlebar using a phone holder, and the application was kept running continuously throughout the experiment (see Fig. 1 for the data acquisition device). Afterward, timestamp alignment was performed through interpolation, and smoothed trajectories together with ground-truth velocities at each epoch were obtained using a Velocity Dead Reckoning (VDR) algorithm. The complete dataset comprises over 25 hours of cycling sensor data covering various road conditions. Data were collected by eight participants using different bicycle models, providing diverse motion patterns and IMU system errors. The dataset was partitioned into 70% for training, 10% for validation, and 20% for testing.

Table 1: Performance Comparison between MoE model and LLIO model

Model	Inference Error	ATE (m)	RTE (m)	Params (M)	FLOPs (M)
LLIO	0.272	4.66	<b>2.30</b>	3.4	49.2
MoE	<b>0.205</b>	4.66	2.36	<b>1.2</b>	<b>8.95</b>



Figure 1: The data acquisition device mounted on a bicycle handlebar.

#### 4.1.2. Evaluation Metrics

To evaluate the localization performance of different methods, we define the following metrics, similar to TLIO.

The **Absolute Translation Error (ATE, m)** measures the root mean square error (RMSE) between the estimated trajectory and the ground-truth trajectory, expressed in meters, and is defined as:

$$\text{ATE} = \sqrt{\frac{1}{n} \sum_{t=1}^n \|p_t^n - \hat{p}_t^n\|^2} \quad (21)$$

where  $p_t^n$  and  $\hat{p}_t^n$  denote the ground-truth and estimated positions at time  $t$ , respectively.

The **Relative Translation Error (RTE, m)** over a given time interval evaluates the relative trajectory error in a locally gravity-aligned coordinate frame. This metric is insensitive to accumulated heading errors. The RTE, measured in meters, is defined as:

$$\text{RTE} = \sqrt{\frac{1}{n} \sum_{t=1}^n \|R_{\text{yaw}}^T (p_t^n - p_{t-\Delta t}^n) - \hat{R}_{\text{yaw}}^T (\hat{p}_t^n - \hat{p}_{t-\Delta t}^n)\|^2} \quad (22)$$

where  $R_{\text{yaw}}$  and  $\hat{R}_{\text{yaw}}$  denote the yaw rotation matrices corresponding to the ground-truth and estimated trajectories, respectively. We use one-minute segments for evaluation, i.e.,  $\Delta t = 1$  minute.

#### 4.2. System Performance

Table 1 presents a performance comparison between the MoE model and its backbone network, namely the ResMLP network, which also serves as the network used in LLIO. The inference error in the table represents the average error of the three-dimensional vectors output by the neural network, defined

as  $\frac{1}{n} \sqrt{\sum \|v_t^n - \hat{v}_t^n\|^2}$ , which is slightly different from the root-mean-square error (RMSE). This metric is used to directly evaluate the inference accuracy of the neural network. The results show that the MoE model achieves comparable performance to the ResMLP network while reducing the number of parameters by 64.7% and the computational cost by 81.8%.

In addition, a subset of trajectories is selected here to directly demonstrate the performance of the MoE algorithm. Fig. 2 illustrates the localization performance of the MoE model on both paved and unpaved road. The MoE model performs better on paved road than on unpaved road, whereas traditional methods based on nonholonomic constraints fail completely on unpaved surfaces.

## 5. Conclusion

In this work, we adopt a learned inertial odometry approach to achieve accurate bicycle localization and introduce a Mixture-of-Experts (MoE) framework to replace the original single-network architecture. Experimental results demonstrate that this method achieves localization accuracy comparable to the LLIO framework while significantly reducing both the number of parameters and computational cost, making it more suitable for deployment on mobile devices. Moreover, the proposed method maintains good performance on unpaved roads, addressing the failure of traditional methods caused by broken incompleteness constraints. This study focuses on architecture-level model lightweighting, and future work will explore techniques such as knowledge distillation to further reduce model size and evaluate deployment on mobile devices.

## References

- [1] Chang, H.W., Georgy, J., El-Sheimy, N., 2015. Improved cycling navigation using inertial sensors measurements from portable devices with arbitrary orientation. *IEEE Transactions on Instrumentation and Measurement* 64, 2012–2019.
- [2] Chen, C., Lu, X., Markham, A., Trigoni, N., 2018. Ionet: Learning to cure the curse of drift in inertial odometry, in: *Proceedings of the AAAI conference on artificial intelligence*.
- [3] Dai, D., Deng, C., Zhao, C., Xu, R., Gao, H., Chen, D., Li, J., Zeng, W., Yu, X., Wu, Y., et al., 2024. Deepseekmoe: Towards ultimate expert specialization in mixture-of-experts language models, in: *Proceedings of the 62nd Annual Meeting of the Association for Computational Linguistics (Volume 1: Long Papers)*, pp. 1280–1297.

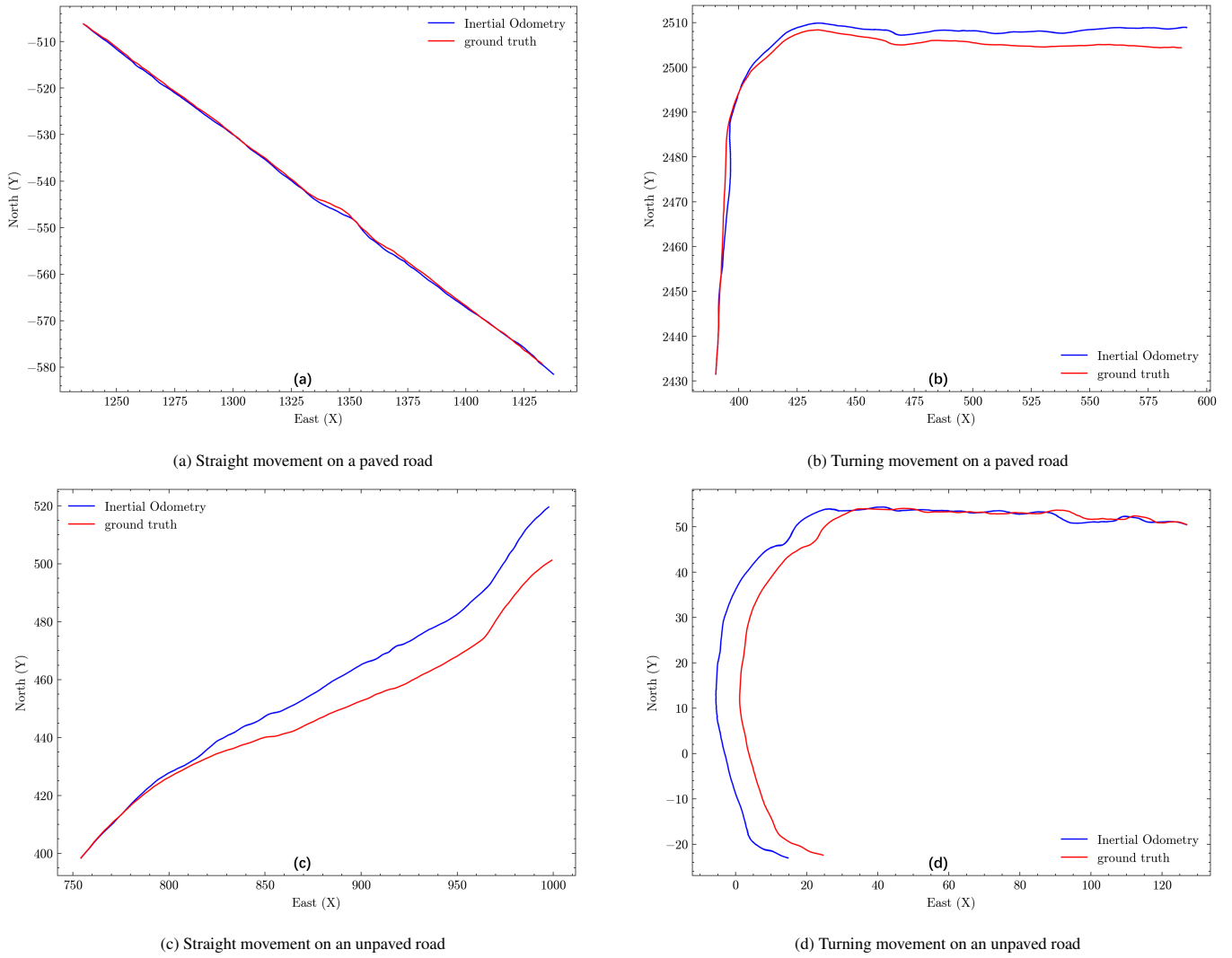


Figure 2: Trajectory visualization under four different conditions.

- [4] Herath, S., Yan, H., Furukawa, Y., 2020. Ronin: Robust neural inertial navigation in the wild: Benchmark, evaluations, & new methods, in: 2020 IEEE international conference on robotics and automation (ICRA), IEEE. pp. 3146–3152.
- [5] Liu, W., Caruso, D., Ilg, E., Dong, J., Mourikis, A.I., Daniilidis, K., Kumar, V., Engel, J., 2020. Tlio: Tight learned inertial odometry. IEEE Robotics and Automation Letters 5, 5653–5660.
- [6] Rao, B., Kazemi, E., Ding, Y., Shila, D.M., Tucker, F.M., Wang, L., 2022. Ctin: Robust contextual transformer network for inertial navigation, in: Proceedings of the AAAI Conference on Artificial Intelligence, pp. 5413–5421.
- [7] Shazeer, N., Mirhoseini, A., Maziarz, K., Davis, A., Le, Q., Hinton, G., Dean, J., 2017. Outrageously large neural networks: The sparsely-gated mixture-of-experts layer, in: International Conference on Learning Representations.
- [8] Touvron, H., Bojanowski, P., Caron, M., Cord, M., El-Nouby, A., Grave, E., Izacard, G., Joulin, A., Synnaeve, G., Verbeek, J., et al., 2022. Resmlp: Feedforward networks for image classification with data-efficient training. IEEE transactions on pattern analysis and machine intelligence 45, 5314–5321.
- [9] Wang, Y., Kuang, J., Niu, X., Liu, J., 2022. Llio: Lightweight learned inertial odometer. IEEE Internet of Things Journal 10, 2508–2518.
- [10] Xiaoji, N., Longyang, D., Jian, K., Yibin, W., 2021. A mems imu and motion constraint-based positioning algorithm for shared bicycles. Journal of Chinese Inertial Technology 29, 300–306. doi:10.13695/j.cnki.12-1222/o3.2021.03.004.